

# Effect of Sterilization Techniques on the Physicochemical Properties of Polysulfone Hollow Fibers

Ben Madsen,<sup>1</sup> David W. Britt,<sup>1</sup> Floyd Griffiths,<sup>1</sup> Elise McKenna,<sup>1</sup> Chih-Hu Ho<sup>2</sup>

<sup>1</sup>Biological Engineering Department, Utah State University, Logan, Utah 84322

<sup>2</sup>Dialyzer R&D Department, Fresenius Medical Care North America, Ogden, Utah 84404

Received 31 October 2009; accepted 19 June 2010

DOI 10.1002/app.32994

Published online 29 September 2010 in Wiley Online Library (wileyonlinelibrary.com).

**ABSTRACT:** Sterilized hollow-fiber membranes are used in hemodialysis, ultrafiltration, bioprocessing, and tissue engineering applications that require a stable and biocompatible surface. In this study, we demonstrated significant changes in the fiber physicochemical properties with different methods of sterilization. Commercial polysulfone (PS) hollow fibers containing poly(vinyl pyrrolidone) were subjected to standard ethylene oxide (ETO), sodium hypochlorite (bleach), and electron-beam (e-beam) sterilization techniques followed by analysis of the surface hydrophilicity, morphology, and water-retention ability. E-beam sterilization rendered more hydrophilic fibers with water contact angles near 47° compared to the ETO- and bleach-treated fibers, which were each near 56°. Atomic force microscopy revealed lumen root mean square (rms) roughness values near 19 nm for all three sterilization methods;

however, e-beam-sterilized and bleach-treated fibers had significantly higher (~ 106 nm) rms values for the outer wall compared to the ETO-sterilized fibers (~ 39 nm). The increased hydrophilicity and surface area of the e-beam-sterilized fiber were reflected by a greater water evaporation rate than that of the ETO-treated fiber. These results demonstrate that common sterilization methods may significantly and distinctly alter the polymer membrane physicochemical properties, which may, in turn, impact the performance and, in particular, surface fouling. For tissue engineering and bioprocessing applications, these changes may be leveraged to promote cell adhesion and spreading. © 2010 Wiley Periodicals, Inc. *J Appl Polym Sci* 119: 3429–3436, 2011

**Key words:** atomic force microscopy (AFM); electron beam irradiation; fibers; surfaces; voids

## INTRODUCTION

The surface physicochemical properties of hollow-fiber membranes (HFMs) are of significant importance as they influence ultrafiltration rates and dictate whether biological components (proteins, cells, bacteria) adsorb to the membrane; these properties may be favorable for cell culture, bioreactor, and tissue engineering applications<sup>1–3</sup> but less desirable in ultrafiltration applications, where biofouling diminishes the filtration efficiency.<sup>4–7</sup> HFM fabrication procedures, including polymer/copolymer and solvent selection, and postfabrication processing and sterilization methods influence the HFM surface chemical and physical properties and impact the overall performance of the membrane.

Polysulfone (PS) and cellulose acetate are the most common materials used in HFM production; they are chosen on the basis of their structural integrity, ease of manufacturing, and biocompatibility. Common copolymer additives include poly(vinyl pyrrolidone) (PVP), poly(vinylidene fluoride), poly(ether

imide), poly(ethylene oxide), and phosphorylcholine polymers.<sup>1,8–12</sup> These copolymers are necessary to form the pore structure in the membrane through phase inversion. Because PS membranes are used in many applications, particular interest has been given to the analysis and modification of membranes containing this polymer and the commonly used hydrophilic additive, PVP. Here, we characterized the physicochemical properties of PS–PVP membranes by following several common sterilization methods.

The influence of sterilization on the HFM properties and performance is of significant importance and may be compounded for multiuse devices subjected to repeated sterilization cycles. As this is the last step before application (or reuse), sterilization is often overlooked. Common biomedical material sterilization methods include steam autoclaving, ethylene oxide (ETO) gas treatment, irradiation, or exposure to several chemical sanitizers, such as sodium hypochlorite, hydrogen peroxide, sodium hydroxide, or ethanol. Here, we focused on ETO, electron-beam (e-beam), and bleach treatments to compare common gas, irradiation, and chemical sterilization methods.

Several methods are frequently used to study membrane properties, including scanning electron microscopy (SEM), atomic force microscopy (AFM), contact angle measurement (CAM), X-ray photoelectron

Correspondence to: D. W. Britt (david.britt@usu.edu).

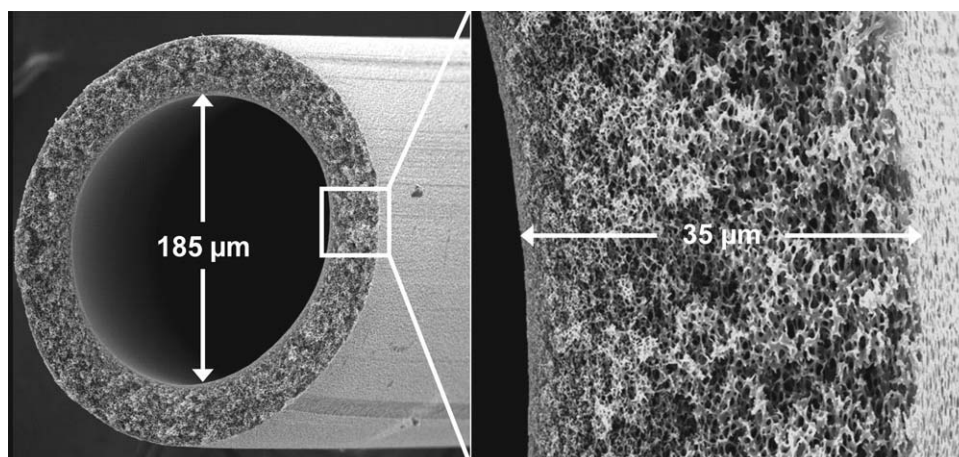


**Figure 1** SEM of the PS-PVP asymmetric dialysis of hollow fibers.<sup>19</sup>

spectrometry, ultrafiltration rate measurements, protein adsorption, and tensile strength testing.<sup>4,8,10–18</sup> We present a direct method for the sectioning of hollow fibers to expose the lumen as a flat surface for CAM and AFM analysis. Additionally, the water evaporation rate measured with a tensiometer force transducer is presented as a sensitive method for characterizing the membrane hydrophilicity and sorption properties.

Applying AFM, CAM, and water evaporation techniques, we demonstrated dramatic changes in the PS HFM surface roughness, hydrophilicity, and water retention as a function of the postfabrication sterilization technique. The results demonstrate that the standard gas, irradiation, and chemical sterilization methods differentially affected the fiber physiochemical properties and can, thus, be selected to fine-tune the material properties toward specific applications.

## EXPERIMENTAL

### Membrane preparation

All HFMs used in this study were prepared by Fresenius Medical Care North America (Ogden, UT). ETO and e-beam-sterilized fibers were obtained from the commercial dialysis cassettes Fresenius Optiflux F200NR and F200NR<sup>c</sup> (Ogden, UT), respectively; each had an aqueous ultrafiltration coefficient (KUF) of  $200 \text{ mL h}^{-1} \text{ mmHg}^{-1}$  and an albumin sieving coefficient of 0.45%. These membranes were manufactured with a polymer blend of PS and PVP.

PS HFMs were fabricated on a pilot line with PS without any other polymer additives. This fiber group was not subjected to any sterilization technique and served only as a control to compare with the PS-PVP membranes. Bleach-treated F200NR fibers were subjected to a 0.57% effective sodium hypochlorite content from the dialysate side at 70°C for 2 min. All HFMs were prepared with the same spinning parameters

(spinneret size, air gap, bore fluid, and rinsing time) to produce asymmetric membranes similar to that shown in Figure 1, with a compact filtering layer at the inner surface and a porous matrix structure through the remainder of the fiber cross section.

Hollow fibers were sectioned to access the lumen for both AFM and CAM with the aid of a stereo microscope (SMZ645, Nikon Corp., Melville, NY). Fibers were fixed on double-sided tape, cut longitudinally with a razor blade, spread open, and rolled flat with a clean glass test tube. Intact fibers were also rolled flat on double-sided tape to present the outside of the fiber as a flat surface.

### Water CAM

The water contact angles (WCAs) of the fibers were measured with a VCA Optima (AST Products, Inc., Billerica, MA). Measurements ( $n = 8$  samples) were made on both the lumen and the outside of the hollow fibers with 0.25- $\mu\text{L}$  droplets of double-distilled water (MP-3A, Barnstead International, Waltham, MA) at 25°C. Statistical analysis was performed on the WCA measurements and all subsequent data sets with two-population  $t$  tests in Origin software (v6.1052, OriginLab Corp., Northampton, MA).

### AFM morphology

The sample surface morphology and roughness were observed with a Bioscope atomic force microscope (Nanoscope IIIa, Digital Instruments, Inc., Santa Barbara, CA) in tapping mode with a silicon nitride cantilever (40 N/m, Tap300, Budget Sensors, Sofia, Bulgaria). A scan size of  $2 \times 2 \mu\text{m}^2$  for the lumen of the fibers was chosen to show the nanostructure of the membranes. A scan size of  $10 \times 10 \mu\text{m}^2$  for the outside of the fibers was chosen to show the macrostructures of the porous membranes. The root mean square (rms) roughness was measured ( $n = 5$ ) with the Nanoscope III imaging software

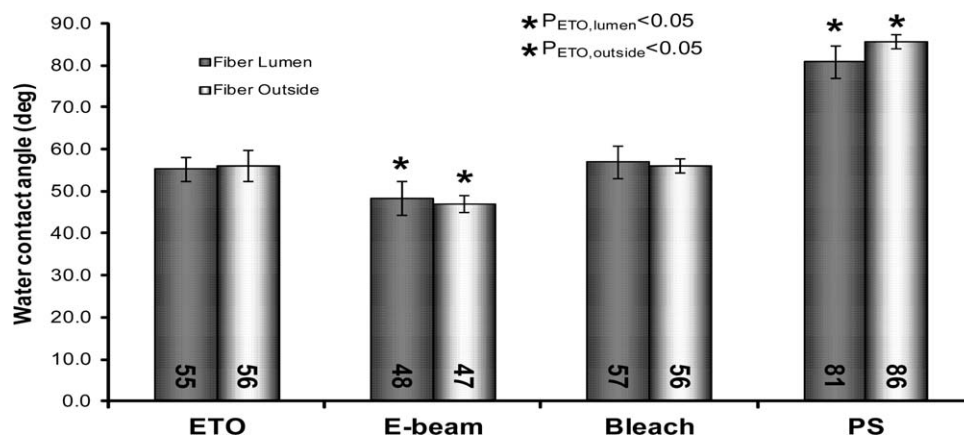


**Figure 2** CAM of the hollow fibers, both lumen (dark) and outside (light; Mean  $\pm$  Standard deviation,  $n = 8$ ). The PS and e-beam-sterilized fibers showed higher and lower contact angles, respectively, than the ETO-sterilized and bleach-treated fibers ( $p < 0.05$ ). The 2-min-bleach-treated fiber had an identical contact angle as the ETO fiber. Fibers bleached for 1 h showed contact angles approaching those of the PS fibers (data not shown). \*P denotes statistical significance for the indicated fibers and surfaces.

(version 5.30r3, Digital Instruments, Inc.). The lumen particle sizes were calculated with a previously described method ( $n \geq 30$ ).<sup>14</sup>

### Water evaporation rate

Water evaporation rates for hollow fibers were obtained with a tensiometer ( $\mu$ trough S, Kibron, Inc., Espoo, Finland). Hollow fibers (1 in. long) were affixed to the tensiometer wire probe with a small piece of double-sided tape, brought into contact with water in a reservoir, and allowed to equilibrate for at least 2 min to reach the maximum absorption capacity (25°C, 24% relative humidity). Upon removal from the water reservoir, the evaporation-induced change in mass was recorded over time. Water evaporation rates for the fibers were calculated from the change in mass over 2-min time periods. This method offered distinct advantages over the use of a standard analytical balance in terms of the sensitivity of the instrument ( $<0.1 \mu\text{g}$ ), instrument equilibration time, and reduced variability due to sample transfer and user error.

## RESULTS

### Surface hydrophilicity as determined by CAMs

CAMs were performed on the lumen and outside of the PS and PS-PVP fibers to compare the wettability of each surface. The results for the CAMs are presented in Figure 2. Statistical analysis was conducted to show significant differences between the outer and lumen contact angles and among the different membrane types. The ETO-sterilized and 2-min-bleach-treated membranes had nearly identical contact angles ( $\sim 56^\circ$ ); this suggested similar fiber surface properties. Longer bleaching times (1 h) significantly increased the contact angle to  $73^\circ$  (data not shown);

this suggested a loss of hydrophilic PVP with time. In contrast, e-beam sterilization led to a significant decrease in WCA ( $\sim 47^\circ$ ) compared to ETO sterilization and bleach treatment ( $p < 0.05$ ). As expected, the pure PS fiber had a significantly higher WCA ( $>80^\circ$ ) than any other membrane because of the lack of PVP. There was no significant difference in WCA between the inner skin and the outer membrane for each fiber type.

### AFM morphology

AFM images of the lumen and outside of each membrane type are shown in Figures 3–6. The images presented here are representative of all of the images taken for each membrane type ( $n = 5$ ). The beadlike structures observed in the lumen images of each membrane type could be classified as nodule aggregates on the basis of the four superimposed tiers of structure in the integrally skinned phase-inversion membranes described by Kesting.<sup>20</sup> *Nodule aggregates* are described as spherical clumps of coalesced macromolecule groups, between which are pores responsible for membrane ultrafiltration characteristics. Nodule aggregate sizes for the lumens of the membranes were as follows ( $n \geq 30$ ): ETO,  $153 \pm 49 \text{ nm}$ ; e-beam,  $97 \pm 32 \text{ nm}$ ; bleach,  $104 \pm 36 \text{ nm}$ ; and PS,  $130 \pm 53 \text{ nm}$ . The nodule aggregate sizes for the ETO and PS membranes were similar, whereas the nodule aggregates for the bleach-treated and e-beam-sterilized fibers were significantly smaller ( $p < 0.05$ ).

The AFM images reported here showed various sizes and structures of the porous membranes, depending on sterilization method. Similar to the trends observed for the lumens, the outsides of the bleach-treated and e-beam-sterilized fibers were significantly different than those of the ETO-sterilized fibers;



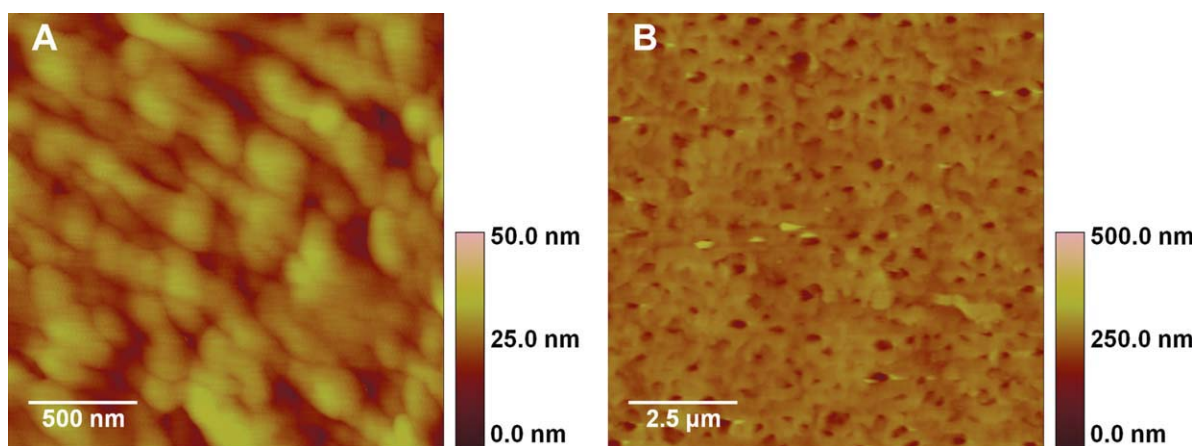


**Figure 3** AFM images of the ETO-sterilized hollow fibers: (A) lumen and (B) outside. The asymmetrical membrane showed nodule aggregates on the lumen and a porous structure on outside. [Color figure can be viewed in the online issue, which is available at [wileyonlinelibrary.com](http://wileyonlinelibrary.com).]

the pore sizes for these membranes were much larger. Also, the outside of the PS membrane exhibited ill-defined pores and a skinlike structure because of the lack of PVP during the phase-inversion process.

The rms roughness of the lumen and outside of each fiber is reported in Figure 7. No significant difference was found among any membranes on the lumen side. However, both the bleach-treated and e-beam-sterilized fibers had significantly higher roughnesses on the outside surfaces compared to the ETO-sterilized and PS fibers. This large increase in the surface roughness arose from the increased pore size, as shown in the AFM images. The large particles observed on the lumen images of both the e-beam-sterilized and bleach-treated membranes were observed in all of the PS–PVP membranes and were included in the calculation of surface roughness.

#### Water evaporation rate

The average evaporation profiles for the sterilized fibers are shown in Figure 8. The calculated evaporation rates of water for the hollow fibers and the mass of water absorbed by the fibers are shown in Table I. Because of the hydrophobic nature of the PS polymer, no water was absorbed by the PS membranes, whereas fibers containing PVP displayed different degrees of water absorption. The e-beam-sterilized fibers exhibited a faster evaporation rate than the ETO-sterilized fibers, whereas the bleach-treated fibers were not significantly different from either the ETO- or e-beam-sterilized fibers. All of the membranes were statistically significant from all of the others in the amount of water absorbed. An increase in the absorbed water could have indicated a larger porosity, whereas a faster evaporation rate likely reflected increased surface area and hydrophilicity.

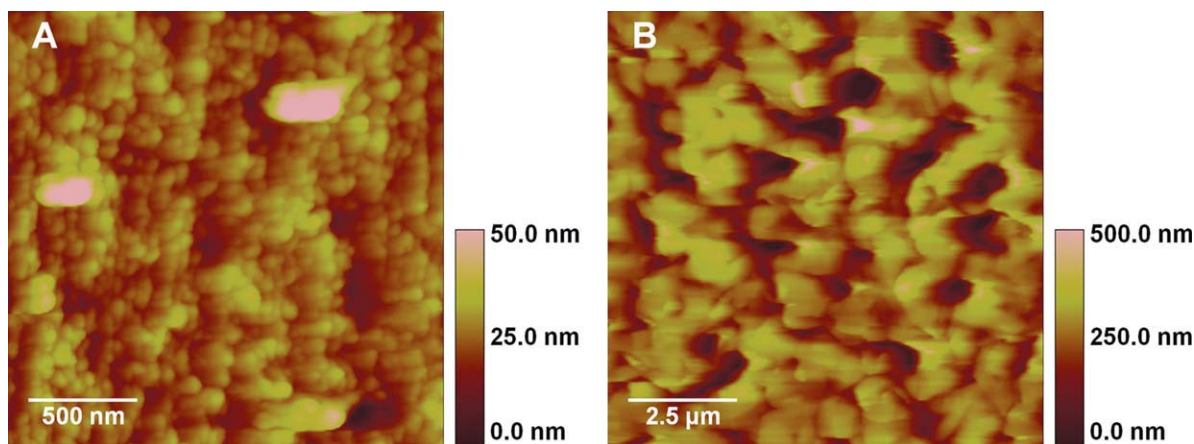


**Figure 4** AFM images of the e-beam-sterilized hollow fibers: (A) lumen and (B) outside. Nodule aggregates for this membrane were significantly smaller than those on the ETO-sterilized membrane. The pores on the outside were also larger than those on the ETO-sterilized membrane. [Color figure can be viewed in the online issue, which is available at [wileyonlinelibrary.com](http://wileyonlinelibrary.com).]

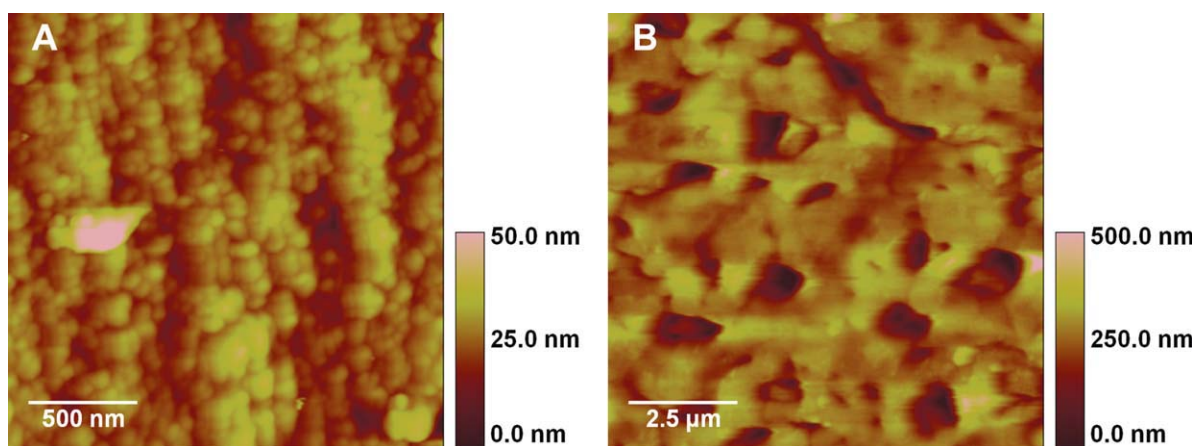


**Figure 5** AFM images of the bleach-treated hollow fibers: (A) lumen and (B) outside. The membrane was structurally very similar to the e-beam-sterilized hollow fibers on both the lumen and the outside. [Color figure can be viewed in the online issue, which is available at [wileyonlinelibrary.com](http://wileyonlinelibrary.com).]

## DISCUSSION

Differential effects of e-beam sterilization, ETO sterilization, and bleach treatment on the PS–PVP membrane physicochemical properties were observed. In particular, the e-beam and 2-min bleach treatments significantly increased the porosity (roughness) of the outer surfaces and decreased the nodule size on the fiber lumens compared to ETO sterilization. Sterilization-induced changes in the membrane contact angles were also observed, with e-beam treatment rendering the fibers more hydrophilic ( $47\text{--}48^\circ$ ) than the ETO and bleach treatments ( $55\text{--}57^\circ$ ). Extended bleach sanitation time beyond 2 min dramatically increased the fiber hydrophobicity, with 1–2 h bleach treatments yielding WCAs approaching that of pure PS ( $81\text{--}86^\circ$ ).<sup>9,21</sup> These results illustrate that the fiber lumen nodule size could be decreased and the outer-wall porosity simultaneously increased with either e-beam or bleach sterilization compared

to ETO sterilization. E-beam sterilization was further distinguished by the production of a more hydrophilic fiber compared to bleach or ETO treatment.

Sterilization methods have the potential to cause slight to major transformations in the membrane chemistry and overall performance, including membrane shrinkage, changes in permeability, increases in pore size, and changes in the surface chemistry and charge,<sup>22–24</sup> of polymeric HFMs. In addition to potentially altering the membrane pore size and ultrafiltration rate, sterilization may also compromise biocompatibility because of changes in the physicochemical properties or the retention of toxic residuals, a concern for ETO.<sup>25,26</sup> Alternatively, modified surface properties may potentially favor cell spreading and proliferation, which is desired in tissue culture applications.<sup>4</sup> The surface roughness and energy are the two primary parameters determining cell–surface interactions. As compared to ETO gas sterilization, both e-beam and bleach treatments increased

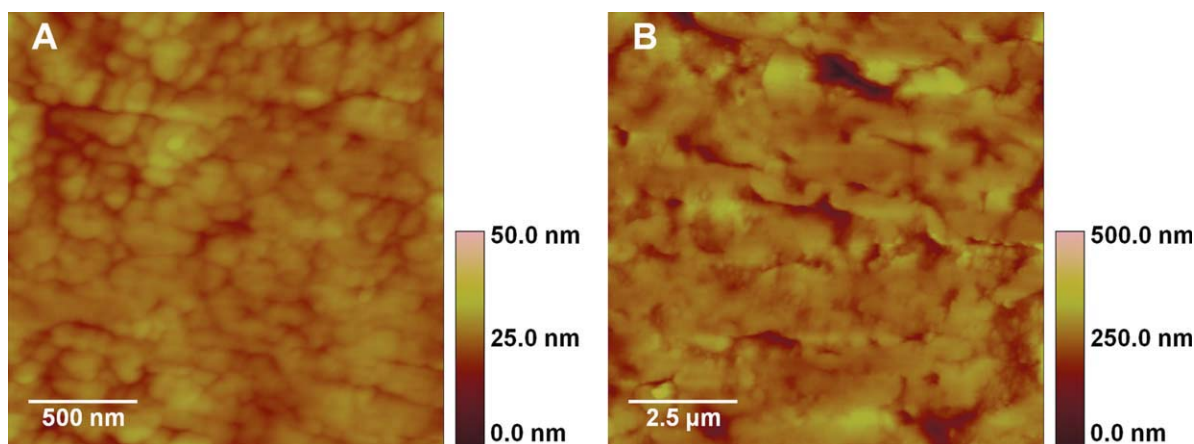


**Figure 6** AFM images of the PS hollow fibers: (A) lumen and (B) outside. The membrane was structurally different, especially on the outside, than other fibers because of the chemical differences of the PS polymer versus the PS–PVP polymer blend. [Color figure can be viewed in the online issue, which is available at [wileyonlinelibrary.com](http://wileyonlinelibrary.com).]

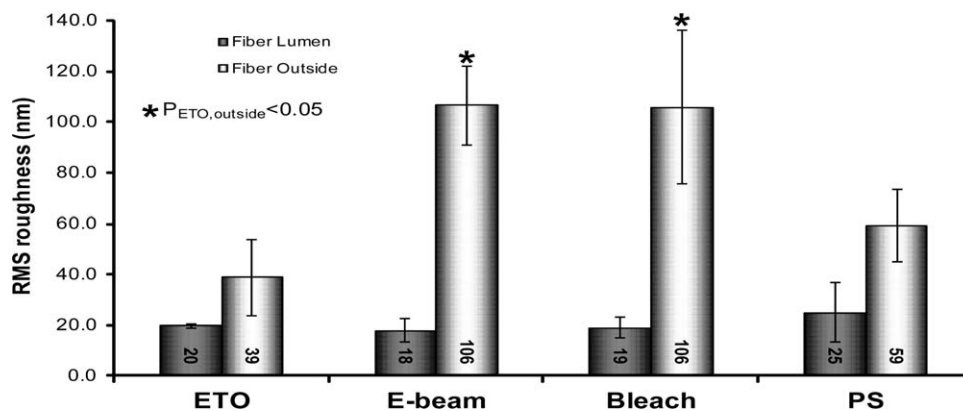


**Figure 7** rms roughness of the hollow fibers, both lumen (dark) and outside (light; Mean  $\pm$  Standard deviation,  $n = 5$ ). No significant difference among the lumen rms values was reported ( $p < 0.05$ ). The bleach-treated and e-beam-sterilized fibers showed significantly higher rms values than the ETO-sterilized and PS fibers. \*P denotes statistical significance for the indicated fibers and surfaces.

the fiber outside-wall rms, decreased the lumen nodule size, and oppositely affected the hydrophobicity in the PS-PVP membranes. Lumen nodules are characteristic features of HFMs, as reported through multiple SEM and AFM investigations.<sup>8,9,13,14,27</sup> The sterilization-induced reduction of nodule size is of concern for HFMs, as the membrane pores reside between nodules, and these surface protrusions may impede pore blockage during the adsorption of macromolecules and cells to the lumen.

It was reported that PS has a high radiation stability under dose conditions as extreme as  $10^4$  kG.<sup>28</sup> Conversely, the e-beam-induced crosslinking of polymers, including PVP, and the restructuring of chemical bonds at lower dosages (10–100 kG) has also been reported.<sup>29–31</sup> The radiation dosage used in this study (25 kG) was on the order of that used to sterilize medical equipment.<sup>32,33</sup> Although 25 kG is approximately 1% of the dosage necessary to reduce the mechanical strength of PS by 50%,<sup>28</sup> the physical and chemical properties of the membranes were indeed altered here. E-beam sterilization in this

study lowered the contact angle for the lumen and outside surfaces by approximately  $8^\circ$  (compared to the ETO-sterilized and bleach-treated membranes) and increased the surface roughness on the outside of the membrane by 2.7 times relative to the ETO-sterilized membrane. Also, the decreased nodule aggregate size compared to the ETO-sterilized membrane may have indicated changes in the polymer-chain interactions. Although the e-beam radiation dosage used in this study was small, it was sufficient to cause slight but significant chemical changes throughout the fiber matrix and physical restructuring on the outside and lumen of the membranes.

The bleaching of HFMs as a sterilization or reprocessing technique has been shown to affect many membrane characteristics, including the surface chemistry, membrane permeability, pore size, and polymer-chain molecular weight.<sup>18,22,34–36</sup> Although reprocessing times often differ on the basis of the technique and end use, the bleaching time of 2 min used in this study was within the time frames tested previously.<sup>35,37,38</sup> It has been shown that PVP is washed from membranes treated with bleach for long periods of time (48 h) because of chain scission via radical reactions<sup>39</sup> and that luminal and outer surface nitrogen contents (due solely to PVP) decrease significantly with bleach times from 1 h.<sup>22</sup>

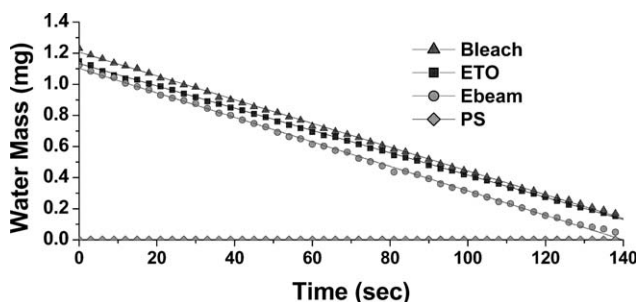


**Figure 8** Average evaporation profiles of the hollow fibers measured by a tensiometer with the mass of absorbed water in the hollow fiber versus time ( $n = 9$ ). The sensitivity of the tensiometer probe allowed for highly accurate measurements ( $<0.1 \mu\text{g}$ ). The error bars were removed for clarity.

**TABLE I**  
Experimental Results for the Water Evaporation Rate and Water Absorption of the Hollow Fibers

Hollow fiber	Absorbed water (mg)	Water evaporation rate ( $\mu\text{g/s}$ )
ETO-sterilized	$1.13 \pm 0.02$	$7.17 \pm 0.56$
E-beam-sterilized	$1.10 \pm 0.04$	$7.88 \pm 0.46$
Bleach-treated	$1.21 \pm 0.02$	$7.64 \pm 0.40$
PS	—	—

$n = 9$ .



We found that 1 h of bleach treatment led to contact angles of  $73.3^\circ$  for the outside of the fibers; this value approached that of the pure PS membranes. Because some PVP was washed out of the bleach-treated membranes, a larger percentage of the membrane surface consisted of the more hydrophobic PS. The results presented here for fibers bleached for 2 min show no significant change in the contact angle of HFMs compared to the ETO fibers; this implied little or no PVP removal from the polymer matrix. Thus, the increased roughness and porosity in the outer membrane and decreased nodule size in the lumen after bleaching was attributed to surface restructuring but not to any significant PVP removal.

HFMs treated with solutions containing bleach for 2 min were shown to increase the clearances of  $\beta_2$ -microglobulin; this suggested increased pore sizes and/or decreased nodule aggregate sizes on the lumen surface of the membrane.<sup>35</sup> Rearrangement of polymer molecules upon bleach treatment may have caused a decrease in the polymer aggregate size, as observed in this study and in previous reports, but left the overall chemistry of the polymer membrane unaffected; this yielded a membrane of equal surface hydrophilicity to the ETO-sterilized membrane.<sup>9,18</sup>

The significant differences in the surface features of the bleach- and e-beam-sterilized fibers compared to the ETO-sterilized fibers were likely due to polymer restructuring associated with these sterilization techniques. Larger pore sizes for the outside of these membranes could have caused an increase in solute transfer and weakening of the fiber structure.<sup>18,22,35</sup> Increased solute transport is of importance in both filtration and cell culture applications, whereas the weakening of the fiber structure is of concern in applications where high trans-membrane pressures are used. However, as previously mentioned, the e-beam dosage of 25 kG used here is around two orders of magnitude below values needed to reduce the fiber mechanical strength by 50%.<sup>28</sup>

HFM water evaporation rates were investigated to further examine the sterilization-induced changes to the fiber surface and bulk properties. Moreover, in cases such as vapor permeation, the ability of a membrane to retain certain liquids, including water, is a key parameter.<sup>40,41</sup> The results presented in Figure 8 and Table I show the initial amount of water absorbed by the fibers and the subsequent evaporation profiles once the fibers were brought out of contact with the water reservoir. Statistical analysis indicated that the mass of water absorbed by each fiber type was significantly different.

Both e-beam and bleach-treated fibers had greater evaporation rates than the ETO-treated fiber; this correlated well to the increased surface roughness of the outer fiber walls observed with AFM for these treatments, as increased rms translated to a greater

surface area for evaporation. The e-beam fiber had the highest evaporation rate, and this coincided well with the increased hydrophilicity of this fiber (contact angle  $\approx 9^\circ$  lower than the other two fibers). This enhanced wicking of water to the interface.

The bleached fiber showed a much greater water-holding capacity compared to the ETO- and e-beam-treated fibers. This may have resulted from a partial breakdown of the matrix of hypochlorite-treated hollow fibers, as reported in SEM micrographs.<sup>34</sup> This phenomenon was not observed for the 25-kG e-beam treatments, which interestingly led to similar increases in rms and decreases in the nodules with bleach treatment (see Figs. 3–7). Evaporation rate analysis is thus seen to be a simple but valuable tool for further characterizing the physicochemical changes induced by sterilization methods, especially when two sterilization methods led to similar changes in the surface topography (e.g., outside-wall rms and lumen nodules).

The sterilization-specific induced changes for PS–PVP HFMs may have specific implications and applications to their fields of use. HFMs used in ultrafiltration, especially hemodialysis, must exhibit specific physicochemical characteristics, including pore size, surface wettability, and biocompatibility. PS–PVP membranes are also increasingly used for cell culture, bioreactors, and tissue engineering because of the ability of the polymer to be formed into specific geometries (i.e., for cell encapsulation). It is, thus, necessary to consider physicochemical changes in these membranes poststerilization. PS–PVP membrane biocompatibility has been attributed to a cushion effect, where an increase in the regularity of polymer structures in wet conditions led to decreased platelet and fibrinogen adhesion.<sup>8,9</sup> The largest increase in platelet adhesion was achieved by more hydrophobic surfaces that had a smaller concentration of PVP at the surface of the membrane. However, it has also been shown that islet cells better adhere to PS and PS–PVP films than to the more hydrophobic polystyrene; this indicated that surface wettability is just one factor affecting cell adhesion to a surface.<sup>4</sup> The importance of minor changes in the interfacial properties to cell and macromolecule binding to surfaces requires that sterilization methods be fully characterized to better anticipate biocompatibility.

## CONCLUSIONS

This study focused on the characterization and comparison of the physicochemical properties of HFMs subjected to several sterilization procedures with CAM, AFM, and water evaporation rate measurement. The e-beam-sterilized fiber exhibited a modest decrease in WCA compared to both ETO-sterilized and bleach-treated membranes and a higher water

evaporation rate than the ETO-sterilized membrane. Also, the e-beam-sterilized and bleach-treated membranes both had larger outside surface rms values and smaller lumen nodule aggregate sizes compared to the ETO-sterilized membrane. These findings indicate significant changes in both the physical and chemical properties of the membrane surfaces and possible changes to the porous matrix for different sterilization techniques. This has significant implications with regard to the selection of sterilization methods because of diverse range of hollow-fiber applications, including ultrafiltration, cell culturing, and tissue engineering. Although detrimental effects to membranes, such as altered mechanical properties, surface antifouling ability, and ultrafiltration, must be considered, sterilization-induced changes to the surface characteristics also provide a facile means for altering the membrane surface roughness and energy, which may be leveraged to promote cell adhesion and spreading for tissue engineering and bioprocessing applications.

## References

- Khayet, M.; Feng, C. Y.; Khulbe, K. C.; Matsuura, T. *Polymer* 2002, 43, 3879.
- Ronco, C.; Ballestri, M.; Brendolan, A. *Blood Purif* 2000, 18, 267.
- Darnige, L.; Legallais, C.; Arvieux, J.; Pitiot, O.; Vijayalakshmi, M. A. *Artif Organs* 1999, 23, 834.
- Beck, J.; Angus, R.; Madsen, B.; Britt, D.; Vernon, B.; Nguyen, K. T. *Tissue Eng* 2007, 13, 589.
- Wolfe, S. P.; Hsu, E.; Reid, L. M.; Macdonald, J. M. *Biotechnol Bioeng* 2002, 77, 83.
- Yang, P.; Teo, W.-K.; Ting, Y.-P. *Bioresour Technol* 2006, 97, 39.
- Ye, S. H.; Watanabe, J.; Takai, M.; Iwasaki, Y.; Ishihara, K. *Biomaterials* 2006, 27, 1955.
- Hayama, M.; Yamamoto, K.-I.; Kohori, F.; Sakai, K. *J Membr Sci* 2004, 234, 41.
- Hayama, M.; Yamamoto, K.-I.; Kohori, F.; Uesaka, T.; Ueno, Y.; Sugaya, H.; Itagaki, I.; Sakai, K. *Biomaterials* 2004, 25, 1019.
- Khayet, M.; Matsuura, T. *Desalination* 2003, 158, 57.
- Hancock, L. F.; Fagen, S. M.; Ziolo, M. S. *Biomaterials* 2000, 21, 725.
- Ye, S. H.; Watanabe, J.; Ishihara, K. *J Biomater Sci Polym Ed* 2004, 15, 981.
- Hayama, M.; Kohori, F.; Sakai, K. *J Membr Sci* 2002, 197, 243.
- Rafat, M.; De, D.; Khulbe, K. C.; Nguyen, T.; Matsuura, T. *J Appl Polym Sci* 2006, 101, 4386.
- Bowen, W. R.; Hilal, N.; Lovitt, R. W.; Williams, P. M. *J Membr Sci* 1996, 110, 233.
- Barzin, J.; Feng, C.; Khulbe, K. C.; Matsuura, T.; Madaeni, S. S.; Mirzadeh, H. *J Membr Sci* 2004, 237, 77.
- Matsuda, M.; Yamamoto, K.-I.; Yakushiji, T.; Fukuda, M.; Miyasaka, T.; Sakai, K. *J Membr Sci* 2008, 310, 219.
- Gaudichet-Maurin, E.; Thominet, F. *J Membr Sci* 2006, 282, 198.
- Henrie, M.; Ford, C.; Andersen, M.; Stroup, E.; Diaz-Buxo, J.; Madsen, B.; Britt, D.; Ho, C.-H. *Artif Organs* 2008, 32, 701.
- Kesting, R. E. *J Appl Polym Sci* 1990, 41, 2739.
- Kim, Y.-W.; Kim, J.-J.; Kim, Y. H. *Korean J Chem Eng* 2003, 20, 1158.
- Wolff, S. H.; Zydney, A. L. *J Membr Sci* 2004, 243, 389.
- Takesawa, S.; Ohmi, S.; Konno, Y.; Sekiguchi, M.; Shitaokoshi, S.; Takahashi, T.; Hidai, H.; Sakai, K. *Nephrol Dial Transplant* 1987, 1, 254.
- Nair, P. D. *J Biomater Appl* 1995, 10, 121.
- Müller, T. F.; Seitz, M.; Eckle, I.; Lange, H.; Kolb, G. *Nephron* 1998, 78, 139.
- Pearson, F.; Bruszer, G.; Lee, W.; Sagona, M.; Sargent, H.; Woods, E.; Dolovich, J.; Caruana, R. *Artif Organs* 1987, 11, 100.
- Khulbe, K. C.; Feng, C. Y.; Matsuura, T.; Mosqueada-Jimenez, D. C.; Rafat, M.; Kingston, D.; Narbaitz, R. M.; Khayet, M. *J Appl Polym Sci* 2007, 104, 710.
- Clough, R. L.; Gillen, K. T.; Dole, M. In *Irradiation Effects on Polymers*; Clegg, D. W.; Collyer, A. A., Eds.; Elsevier: New York, 1991.
- Jiang, B.; Wu, Z.; Zhao, H.; Tang, F.; Lu, J.; Wei, Q.; Zhang, X. *Biomaterials* 2006, 27, 15.
- Kim, C. O.; Kim, D. H.; Kim, J. S.; Park, J. W. *Langmuir* 2006, 22, 4131.
- Meinhold, D.; Schweiss, R.; Zschoche, S.; Janke, A.; Baier, A.; Simon, F.; Dorschner, H.; Werner, C. *Langmuir* 2004, 20, 396.
- Clough, R. L. *Nucl Instrum Methods B* 2001, 185, 8.
- Hagman, D. E. In *Remington: The Science and Practice of Pharmacy*; Troyand, D. B.; Beringer, P., Eds.; Lippincott Williams & Wilkins: Baltimore, MD, 2005.
- Rouaix, S.; Causserand, C.; Aymar, P. *J Membr Sci* 2006, 277, 137.
- Cheung, A. K.; Agodoa, L. Y.; Daugirdas, J. T.; Depner, T. A.; Gotch, F. A.; Greene, T.; Levin, N. W.; Leypoldt, J. K. *J Am Soc Nephrol* 1999, 10, 117.
- Qin, J.-J.; Wong, F.-S. *Desalination* 2002, 146, 307.
- Gagnon, R.; Kaye, M. *Clin Nephrol* 1985, 24, 21.
- Murthy, B.; Sundaram, S.; Jaber, B.; Perrella, C.; Meyer, K.; Pereira, B. *J Am Soc Nephrol* 1998, 9, 464.
- Wienk, I. M.; Meuleman, E. E. B.; Borneman, Z.; Boomgaard, T. V. D.; Smolders, C. A. *J Polym Sci Part Polym Chem Ed* 1995, 33, 49.
- Shi, B.; Wu, Y.; Liu, J. *Desalination* 2004, 161, 59.
- Fu, Y.-J.; Hu, C.-C.; Lee, K.-R.; Lai, J.-Y. *Desalination* 2006, 193, 119.